IEEE Access
Multidisciplinary ⋮ Rapid Review ⋮ Open Access Journal

Received 6 March 2023, accepted 16 March 2023, date of publication 23 March 2023, date of current version 28 March 2023.

Digital Object Identifier 10.1109/ACCESS.2023.3261126

RESEARCH ARTICLE

Research on Transient Low-Frequency Oscillation of Electrified Railway Vehicle-Grid Coupling System

ZHIYONG LI[1], JIAHUA PI[1], YUAN CAO[1], YEFAN WU[2], AND ZHIJIE JIA[3]
[1]School of Automation, Central South University, Changsha 410083, China
[2]Economic & Technical Research Institute, State Grid Hunan Electric Power Company Ltd., Changsha 410029, China
[3]State Grid Anhui Ultra High Voltage Company Ltd., Hefei 230022, China

Corresponding author: Jiahua Pi (214612235@csu.edu.cn)

This work was supported in part by the National Natural Science Foundation of China under Grant 61973322 and Grant 62103443, and in part by the Hunan National Natural Science Foundation under Grant 2002JJ40630.

ABSTRACT At the moment of electric locomotive passing the neutral-section, the voltage and current of traction network may have low-frequency oscillation (LFO), which will seriously affect the safe operation of the railway. Aiming at eliminating the transient LFO, a modeling method of vehicle-grid coupling system based on flux-current theory is presented in this paper. In the model of electric locomotive, the transient current control strategy and magnetic saturation of on-board transformer are considered, and the equivalent model of excitation inductance of on-board transformer is established based on the flux-current theory. Using this model, based on the Middlebrook impedance ratio criterion, the stability region of vehicle-grid coupling system is analyzed under the influence of average saturation of on-board transformer and control parameters of electric locomotive. The simulation results are analyzed to evaluate and verify the proposed modeling method of LFO. This work has the benefits of defining the opening and closing phase angle region of system stability as well as providing guidance to adaptively modify the control parameters to suppress the LFO.

INDEX TERMS Electrified railways, impedance ratio criterion, low-frequency oscillation, stability region, vehicle-grid coupling system.

NOMENCLATURE

C_d	Voltage stabilizing capacitor.
I_{N1}	Output current of the voltage loop.
I_{N2}	Effective component of the given current at the DC side.
I_{kST}	Critical saturation currents.
I_m	Excitation current of on-board transformer.
I_n^*	Given value of the network side current.
i_d	DC link current.
i_n	Output current at secondary side of on-board transformer.
i_s	Current of traction network.
K_{ip}	Proportional parameter of the current loop regulator.
K_{vi}	Integral parameter of the voltage loop regulator.
K_{vp}	Proportional parameter of the voltage loop regulator.
k_b	Saturation of on-board transformer.
$\bar{k}_b$	Average saturation of on-board transformer.
$L_{1\sigma}$	Equivalent inductance of the primary winding of on-board transformer.
$L_{2\sigma}$	Equivalent inductance of the secondary winding of on-board transformer.
L_m	Excitation inductance of on-board transformer.
L_{mb}	Equivalent inductance in nonlinear region.
L_{mdy}	Equivalent inductance of transformer in one cycle.
L_{mx}	Equivalent inductance in linear region.
R_d	Equivalent impedance of electric locomotive load.
$\bar{S}_{ab}$	Average value of the difference between the switching functions, generally 0.5.
T	PWM switching period.
U_d^*	Given value of DC side voltage.

The associate editor coordinating the review of this manuscript and approving it for publication was Diego Bellan.

u_N Voltage of on-board transformer.
u_{ab} Modulating signal.
u_s Voltage of traction network.
u_d DC voltage at the output terminal of the rectifier.
u_n Output voltage at secondary side of on-board transformer.
Z_0 Front output impedance of cascade system.
Z_c Equivalent impedance of capacitance to ground.
Z_{eq} Equivalent impedance of the traction network line.
Z_{inb} Equivalent input impedance of the electric locomotive when transformer is saturated.
Z_{ind} Rear input impedance of cascade system.
Z_{inx} Equivalent input impedance of the electric locomotive when transformer is not saturated.
Z_p Equivalent impedance of rectifier input side.
Z_T Equivalent impedance of traction transformer.
α Closing phase angle of on-board transformer.
β Opening phase angle of on-board transformer.
ϕ Flux of on-board transformer.
ϕ'_L Magnetic flux corresponding to inductance in the flux-current model.
ϕ_m Amplitude of steady-state flux of on-board transformer.
ϕ'_R Magnetic flux corresponding to resistance in the flux-current model.
ϕ_r Residual magnetism of on-board transformer.
ϕ_S Steady-state flux of on-board transformer.
ϕ'_S Magnetic flux corresponding to grid voltage in flux-current model.
ϕ_{ST} Magnetic flux at both ends of on-board transformer in the flux-current model.
ϕ_{sat} Critical saturated flux.
ϕ_T Transient flux of on-board transformer.
ϕ'_T Magnetic flux at both ends of the traction transformer.
ϕ_{Tc} Initial value of transient flux of on-board transformer.

I. INTRODUCTION

Electrified railway is an important part of comprehensive transportation hub, which has been supported and vigorously developed by countries all over the world [1], [2], [3], [4]. When the electric locomotive passes the neutral-section, there will be a complex electromagnetic transient process. When the electric locomotive adopts manual or on-board automatic passing, the on-board transformer may produce a large inrush current when it is closed without load, causing the voltage and current of the vehicle-grid coupling system to oscillate [5], [6], [7]. This will cause train traction blockade and feeder protection malfunction of traction substation, which seriously affects train operation safety [8], [9], [10], [11], [12]. Table 1 shows the LFO phenomena in the railway systems of various countries in the world since 2006 [13], [14]. These cases have caused the problem that electric locomotives can not enter or leave normally, which has caused great harm to the stability and safety of the railway system.

TABLE 1. LFO cases in electrified railways.

Case Number	Frequency (Hz)	Time (Year)	Locations
1	7	2006	Siemens test, Germany
2	5	2008	Thionville, France
3	5	2010	Qingdao, China
4	6~7	2011	Shanhaiguan Hub, China
5	2	2014	Xuzhou North Hub, China

Taking a traction substation of Beijing-Guangzhou high-speed line as an example, the field measured data show that the electric locomotive is prone to cause LFO during the neutral-section passing, and the catenary voltage fluctuates sharply after the oscillation, which seriously endangers the safe operation of the electrified railway. In this paper, the mechanism of LFO caused by electric locomotive passing the neutral-section is analyzed.

The vehicle-grid coupling system of electrified railway is a dynamic coupling chain combination network with multi-source and multi-load, including traction power supply system model and electric locomotive model.

For the establishment of the traction power supply system model, references [15], [16], and [17] regards the traction network as a passive linear system, and based on Thevenin's theorem, the impedance of the traction power supply system is equivalent to the series connection of resistance and inductance. In reference [18], the influence of traction network on ground capacitance is considered in the equivalence of traction power supply system, and the impedance of traction network is simplified as the parallel connection of line impedance, transformer impedance and distributed capacitance. Reference [19] developed a harmonic generator based on the frequency scanning method, and obtained the (inter)harmonic impedance of railways through experimental measurement. Based on the equivalent circuit model of traction network, reference [20] established the flux-current loop model of traction power supply system by considering the integral relationship between flux and voltage, and analyzed the generation mechanism and influencing factors of inrush current electric locomotive passes the neutral-section.

For the establishment of the electric locomotive model, reference [21] regards the electric locomotive running at a constant speed as a constant power load and equates it to a current source. This method is only applicable to the electric locomotive running normally, and cannot reflect the influence of the control strategy of the electric locomotive. In reference [22], the vehicle-grid interaction mechanism and equivalent modeled all frequency impedance behaviors of electric locomotives and traction networks is studied. In most modeling methods, the on-board transformer is simply equivalent to the leakage inductance, which is only applicable to the steady-state operation of electric locomotive, and cannot analyze the transient phenomenon of electric locomotive when it passes

the neutral-section. In order to study the transient problem, some scholars have proposed a method to establish the flux current loop model. Based on the flux-current loop model, references [23] and [24] constructed an equivalent model of electric locomotive when it passes the neutral-section, and analyzes the saturation characteristics of on-board transformers under different conditions. This model can reasonably explain the generation mechanism and attenuation characteristics of magnetizing inrush current and sympathetic inrush current, and provides a new idea for analyzing the LFO caused by electric locomotive passing the neutral-section.

The LFO in electrified railway is the root cause of stability issue occurring in vehicle-grid coupling system. Any oscillation problem can be attributed to the impedance problem. At present, there are two mainstream stability analysis methods of vehicle-grid coupling system: eigenvalue analysis based on state space formula [25], [26], [27] and impedance analysis based on frequency domain model [28], [29], [30], [31], [32].

The first method is to describe the impedance problem with the formula of state, and transform the stability analysis of the vehicle-grid coupling system into the eigenvalue problem. Reference [25] described how a traction power system and its dynamical railway-related components are modelled in a commercially available power system analysis software and studied by linear analysis such as eigenvalues, participation factors and parameter sensitivities. In reference [26], the entire single-phase railway power supply including the vehicle is modelled together in the time-invariant rotating reference frame. Such a reference-frame transformation allows utilization of linearization tools as eigenvalue analysis including participation factors and parameter sensitivity analysis. Reference [27] proposed a method combining time-domain simulation with eigenvalue analysis, and analyzed the influence of various parameters on LFO. In general, the eigenvalue method can accurately identify the oscillation mode of the vehicle-grid coupling system, and obtain the damping ratio and LFO frequency of the system, but the calculation of this method is usually cumbersome, and the influence of closing phase angle and remanence of on-board transformer on flux is not considered when the electric locomotive passes the neutral-section.

The other method is to use the impedance characteristics of the system in the frequency domain to analyze the transfer function and judge the stability of the system according to its dominant poles. In reference [28], the stability of vehicle-grid coupling system is analyzed by utilizing Middlebrook impedance ratio criterion, but only the current inner loop is considered for the rear input impedance of cascade system. In reference [29], the LFO factors including the control parameters, line impedance, load and number of locomotives in frequency domain is analyzed, and the frequency domain analysis results are effectively verified by time domain simulation. In reference [30], the impedance model of vehicle-grid coupling system is established, and the generalized Nyquist analysis method is used to analyze

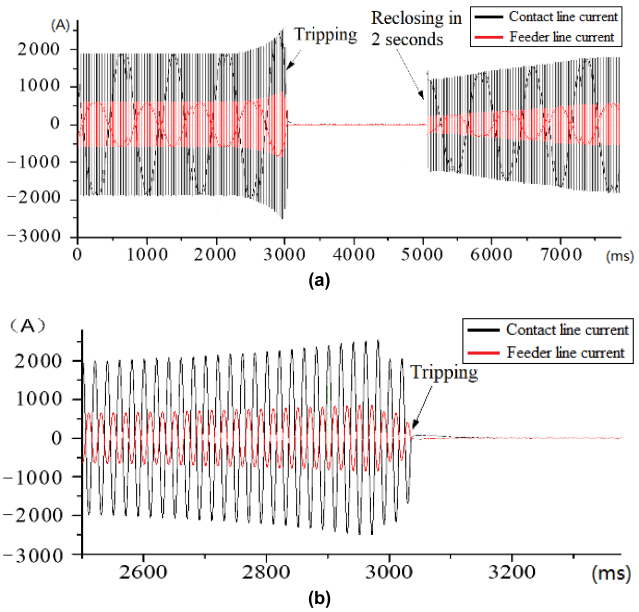

FIGURE 1. Measured waveforms before and after tripping. (a) overall waveforms (b) zoom-in view of waveforms from 2500 to 3500ms.

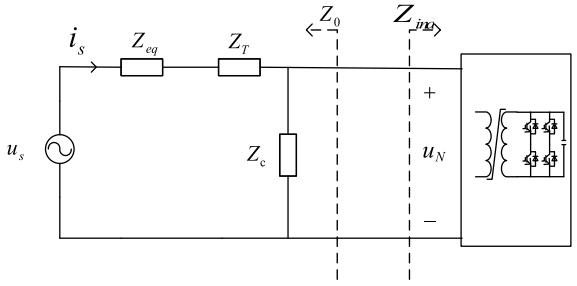

FIGURE 2. Equivalent model of vehicle-grid coupling system.

the stability of the system. In reference [31], a new stability criterion based on forbidden region is proposed to analyze the stability of the system for the dq decoupled multi-input multi-output vehicle-grid coupling system, which is more conservative. Reference [32] predicted the stability of LFO based on the analysis of dominant poles, and verified that this method is faster in predicting low-frequency instability through simulation and experiments. The feature of impedance analysis method is black box modeling, in another word, analysis is carried out without detailed system parameters. The equivalent model of the converter is established according to the frequency domain transfer function, and then converted into impedance. The impedance analysis method can use some traditional linear system analysis methods, such as Bode diagram and root locus, to analyze the stability of the vehicle-grid coupling system, which is widely used. However, the above stability analysis does not consider the influence of the nonlinear characteristics of the transformer and the transient flux when the electric locomotive passes the neutral-section. In the practical project, the transformer may be in the saturated nonlinear working area, so the linear steady

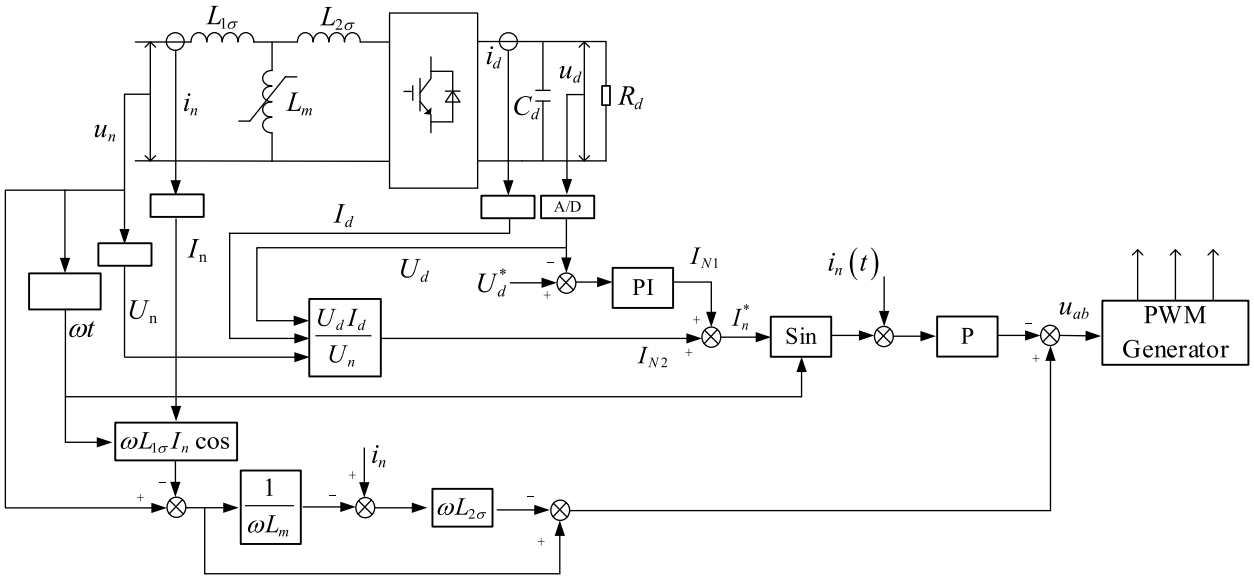

FIGURE 3. Structure diagram of electric locomotive system with control loop.

state analysis method cannot be directly used to analyze the transient LFO.

To sum up, the LFO of electric locomotive when passing the neutral-section is affected by three characteristics: transformer nonlinearity, initial state uncertainty, and control parameters of electric locomotive. The uncertainty of the initial state is related to the closing phase angle and remanence of the on-board transformer when the electric locomotive passing the neutral-section.

In order to address the issues described above, this paper evaluates the transient LFO of electrified railway vehicle-grid coupling system. The main contributions of this paper can be summarized as:

(1) A modelling method of vehicle-grid coupling system is presented based on the flux-current theory to analyze the magnetic saturation of on-board transformer. As a result, the accurate estimation of transient inductance can be achieved.

(2) The system stability region is determined when the electric locomotive passes the neutral-section, and the opening and closing phase angle region that makes the system stable is defined.

(3) A simulation platform is built in Simulink to verify the correctness of the analysis. This work can provide guidance to adaptively modify the control parameters to suppress the LFO.

II. MODEL ESTABLISHMENT OF VEHICLE-GRID COUPLING SYSTEM

Fig. 1 shows an example current measured waveforms before and after tripping. It can be seen from Fig. 1(a) that the current has an obvious upward trend, and from Fig. 1(b) that the current increases rapidly from 2500 to 3000ms, with an oscillation trend. As the tripping time is close and most of the locomotive are of the same model, this paper considers that the tripping is caused by the LFO generated by electric locomotive when passing the neutral-section. It should be noted that the curve shown in Fig. 1 only contains the operation data under stable condition for the practical system, while the instability is not illustrated for safety reason. However, the unstable condition can be verified through theoretical analysis and simulation. Missing data of unstable part in Fig. 1 shall not impact the proposed control/modeling analysis or any other discussion through the paper.

Aiming at the above problems, this paper analyzes the LFO generated when the electric locomotive passes the neutral-section. According to the Thevenin equivalent circuit, the traction network can be equivalent to the parallel connection of impedance and capacitance. Convert the traction network model to the secondary side of the traction transformer and the electric locomotive model to the primary side of the locomotive transformer. The circuit model of the vehicle-grid coupling system is established as shown in Fig. 2. The vehicle-grid coupling system can be equivalent to a cascade system, which includes the front output module (traction power supply network) and the rear output module (electric locomotive load).

Wherein, u_s is the voltage of traction network, i_s is the current of traction network, Z_{eq} is the equivalent impedance of the traction network line, Z_T is the equivalent impedance of traction transformer, Z_c is the equivalent impedance of capacitance to ground, Z_0 is the front output impedance of cascade system, Z_{ind} is the rear input impedance of cascade system, u_N is the voltage of on-board transformer.

The front output impedance expression of cascade system is:

$$Z_o = \frac{Z_c\left(Z_T + Z_{eq}\right)}{Z_c + Z_T + Z_{eq}} \tag{1}$$

The equivalent impedance of electric locomotive includes on-board transformer, and the on-board transformer will become saturated when the electric locomotive passes the neutral-section. At this time, the influence of nonlinear excitation inductance cannot be ignored. Therefore, the nonlinear problem of the on-board transformer will be considered below to establish the electric locomotive model.

A. ELECTRIC LOCOMOTIVE CIRCUIT MODEL WITH NONLINEAR T-NETWORK INTERFACE

1) MAIN CIRCUIT AND CONTROL STRATEGY OF ELECTRIC LOCOMOTIVE

The rectifier of the electric locomotive adopts multiple two-level technology. In order to facilitate the research, the single pulse rectifier is analyzed first. Ignoring the secondary filtering circuit, the electric locomotive controller adopts transient current control strategy. The structure diagram of the electric locomotive including the control system is shown in Fig. 3.

Wherein, u_n is the output voltage at secondary side of the on-board transformer, that is, the equivalent voltage converted from the catenary to the secondary side of the on-board transformer, i_n is the output current at secondary side of on-board transformer, L_m is the excitation inductance of on-board transformer, $L_{1\sigma}$ is equivalent inductance of the primary winding of on-board transformer, $L_{2\sigma}$ is the equivalent inductance of the secondary winding of on-board transformer, i_d is the DC link current, C_d is the voltage stabilizing capacitor, u_d is the Dc link voltage, R_d is the equivalent impedance of electric locomotive load, U_d^* is the given value of DC side voltage, I_{N1} is the output current of the voltage loop, I_{N2} is the effective component of the given current at the DC side, I_n^* is the given value of the network side current and u_{ab} is the modulating signal. In the transient current control strategy, the instantaneous phase ωt of the grid side voltage u_n is obtained through phase locked loop (PLL).

As shown in Fig. 3, the mathematical model of transient current control is:

$$\begin{cases} I_{N1} = K_{vp}\left(U_d^* - U_d\right) + K_{vi}\int\left(U_d^* - U_d\right)dt \\ I_{N2} = \dfrac{I_d U_d}{U_n} \\ I_n^* = I_{N1} + I_{N2} \\ u_{ab} = u_n - \omega L_{1\sigma} I_n \cos\theta - \\ \left(i_n - \dfrac{u_n - \omega L_{1\sigma} I_n \cos\theta}{\omega L_m}\right)\omega L_{2\sigma} \\ -K_{ip}\left[I_n^* \sin(\omega t) - i_n(t)\right] \end{cases} \tag{2}$$

wherein, K_{vp} is the proportional parameter of the voltage loop regulator, K_{vi} is the integral parameter of the voltage loop regulator and K_{ip} is the proportional parameter of the current loop regulator.

2) EQUIVALENT IMPEDANCE OF ELECTRIC LOCOMOTIVE

The equivalent impedance of electric locomotive involves the control link of rectifier, and its control block diagram is shown in Fig. 4.

In Fig. 4, G_1 is the sampling delay link, G_2 is the current loop proportional link, G_3 is the transfer function of Pulse Width Modulation (PWM) modulation, G_5 is the voltage loop proportional integral link, T is the PWM switching period, and $\bar{S}_{ab}$ is the average value of the difference between the switching functions, generally 0.5. Taking u_n as input and i_n as output, the equivalent impedance of rectifier in frequency domain is:

$$\begin{aligned} Z_p(s) &= \frac{1}{\frac{i_n}{u_n}} \\ &= \frac{1 + G_4G_9 + G_8G_9 + G_1G_2G_3G_4\left(G_1G_5G_6G_7 + 1\right)}{G_4 + G_8 - G_1G_3G_4} \end{aligned} \tag{3}$$

The electric locomotive has four power carriages, and each power carriage uses a dual two-level pulse rectifier. Therefore, the equivalent impedance of the electric locomotive is:

$$Z_{ind}(s) = \frac{k^2}{8} Z_p(S) \tag{4}$$

B. EQUIVALENT MODEL OF EXCITATION INDUCTANCE OF ON-BOARD TRANSFORMER BASED ON FLUX-CURRENT LOOP

L_m is a non-linear inductance, and its value cannot be obtained directly. The value of L_m is related to the flux at both ends of the transformer.

$$L_m = f(i, \phi) \tag{5}$$

Considering the relationship between the flux and the current at both ends of the transformer, the equivalent excitation inductance model of on-board transformer is established as follows.

The load on the secondary side of the on-board transformer will be cut off and run without load at the moment of passing the neutral-section. For the transformer, the relationship between the magnetic induction strength and the magnetic field strength is nonlinear, with hysteresis and saturation characteristics. According to Maxwell's formulas, the relationship between transformer flux and excitation current is shown in Fig. 5(a) without considering the change of transformer coil turns and cross-sectional area.

If we do not consider the time-delay characteristics, we can perform piecewise linearization on Fig. 5(a), and the results are shown in Fig. 5(b). The curve can be divided into three parts: linear region, positive saturation region and negative saturation region. Abscissa I_m is the excitation current of on-board transformer, and ordinate ϕ_{ST} is the magnetic flux at both ends of on-board transformer. I_{kST} is the critical saturation currents, ϕ_{sat} is the critical saturated flux, L_{mx} and L_{mb} are the equivalent inductors in linear region and nonlinear region respectively. When the on-board transformer is in the linear region, the excitation current and the magnetic flux at both ends of the on-board transformer are less than the critical saturation point, and the excitation inductance is L_{mx}; When the transformer is in the positive or negative saturation region,

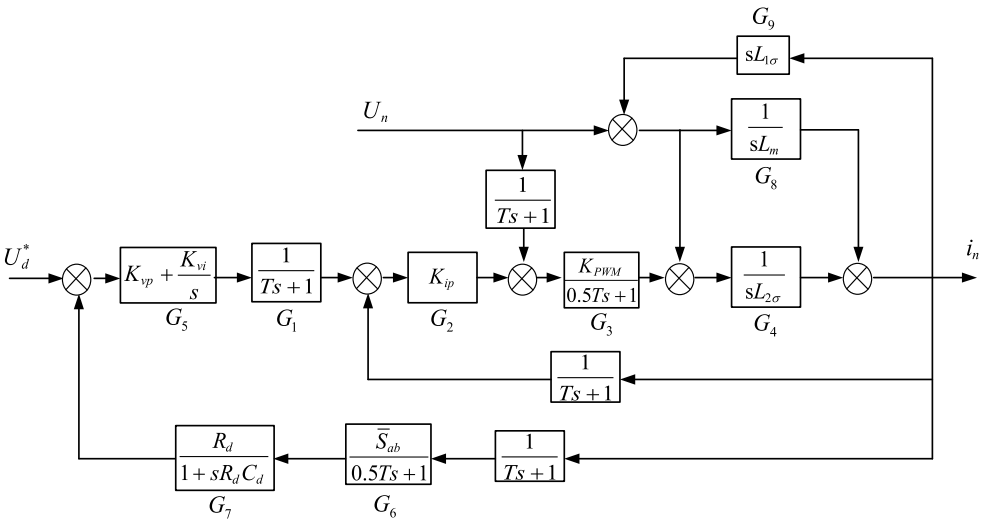

FIGURE 4. Control block diagram of grid side rectifier.

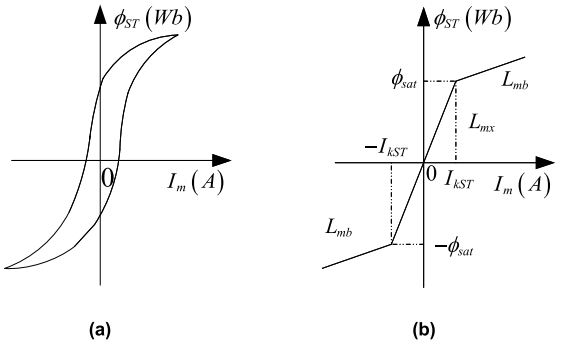

FIGURE 5. Flux current characteristics of transformer. (a) hysteresis current characteristics (b) linearized flux current curve.

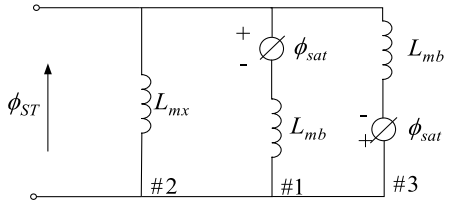

FIGURE 6. Flux-current equivalent model of transformer.

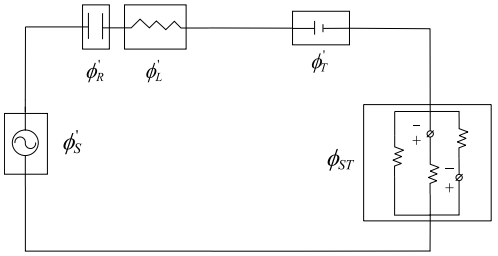

FIGURE 7. Equivalent model of excitation inductance for on-board transformer.

the excitation current and the magnetic flux at both ends of the transformer are greater than the critical saturation point, and the excitation inductance is L_{mb}.

The mathematical expression of flux-current loop of the on-board transformer is:

$$\phi_{ST} = \begin{cases} L_{mb}\left(I_{ST} + \dfrac{\phi_{sat}}{L_{mx}}\right) - \phi_{sat} \ (\phi_{ST} < -\phi_{sat}) \\ L_{mx} I_{ST} (-\phi_{sat} < \phi_{ST} < \phi_{sat}) \\ L_{mb}\left(I_{ST} - \dfrac{\phi_{sat}}{L_{mx}}\right) + \phi_{sat} \ (\phi_{ST} > \phi_{sat}) \end{cases} \tag{6}$$

The flux-current loop model of the on-board transformer is established by formula (6), as shown in Fig. 6. Branch # 2 is always on, and the on-board transformer is in the linear region. When the flux exceeds the critical saturation flux from the positive or negative direction, branch # 1 or # 3 is opened, which is equivalent to the transformer working in the positive saturation area or negative saturation area.

The flux at both ends of the on-board transformer will gradually decay, and the decay speed is related to the line parameters. Therefore, it is necessary to establish the flux-current model of the traction power supply system. By analogy with the modeling method of the transformer, the models of the grid voltage, the resistance and the inductance of the traction network in the traction power supply system are established, which together form the equivalent excitation inductance model of the on-board transformer, as shown in Fig. 7.

In Fig. 7, ϕ_S' is the magnetic flux corresponding to grid voltage in flux-current model, ϕ_R' is the magnetic flux corresponding to resistance in the flux-current model, ϕ_L' is the magnetic flux corresponding to inductance in the flux-current model and ϕ_T' is the magnetic flux at both ends of the traction transformer.

The resistance has the property of ''magnetic storage'' in the flux-current model, so the resistance symbol in the flux-current loop can be represented by the capacitance symbol in the circuit. The flux of the inductance is proportional to the current, which is similar to the resistance characteristic in the voltage-current circuit. Therefore, the symbol of the inductance in the flux-current circuit can be replaced by the resistance symbol in the circuit. In order to distinguish the components in the circuit model and the flux-current loop model, the flux-current loop components are uniformly framed. The model can analyze the transient flux change in transient phase and the influence of transient flux on on-board transformer, which lays a foundation for analyzing the influence of the transient flux change of on-board transformer on the equivalent impedance of electric locomotive.

III. MECHANISM ANALYSIS OF TRANSIENT LFO

The impedance ratio criterion is widely used in LFO analysis. However, this method can only analyze the steady-state stability, and cannot directly analyze the nonlinear problem caused by the equivalent impedance change of the on-board transformer when the electric locomotive passes the neutral-section. To solve this problem, this section considers the initial state when the on-board transformer is closed, analyzes the influence of the electric locomotive passing the neutral-section on the equivalent impedance of the on-board transformer based on the flux-current loop model, derives the function of the saturation of the on-board transformer changing with time, and turns the nonlinear problem into a time-varying problem. The average saturation of the on-board transformer in different time periods is calculated based on the sliding window theory, and the transient problem is averaged by sections. Then, the stability of the vehicle-grid coupling system is analyzed based on the Middlebrook impedance ratio criterion, the generation mechanism and oscillation frequency of LFO are clarified, the stability region of the vehicle-grid coupling system under the influence of the main parameters is determined, and the opening and closing phase angle under the stability of vehicle-grid coupling system is defined.

A. ANALYSIS OF EQUIVALENT EXCITATION INDUCTANCE

According to the excitation inductance equivalent model of on-board transformer in Fig. 7, the flux at both ends of the transformer of the electric locomotive is formed by the superposition of the steady-state flux and the transient flux corresponding to the closing moment, as shown in formula (7).

$$\phi = \phi_S + \phi_T \tag{7}$$

wherein, ϕ is the flux of on-board transformer, ϕ_S is the steady-state flux of on-board transformer and ϕ_T is the transient flux of on-board transformer.

The initial value ϕ_{Tc} of ϕ_T is affected by the closing phase angle α and residual magnetism ϕ_r of the on-board transformer. The relationship between the initial value of transient flux and the closing phase angle and residual magnetism is shown in formula (8).

$$\phi_{Tc} = \phi_m cos\alpha + \phi_r \tag{8}$$

wherein, ϕ_m is the amplitude of steady-state flux of on-board transformer. The transient flux will gradually decay over time. It can be seen from Fig. 7 that the impedance of the traction network in the flux-current circuit is equivalent to capacitance and resistance, in which the capacitance has the characteristics of ''magnetic storage''. By analogy to the attenuation curve of the capacitor voltage in the RC circuit, the transient flux will decay exponentially. As the line parameters of the traction network do not change, the closing phase angle and residual magnetism do not affect the attenuation trend of the transient magnetic flux when they affect the magnitude of the transient magnetic flux. The transient flux attenuation is analyzed when the closing phase angle is 0 degrees and the remanence is 1 p.u. The transient flux attenuation curve is shown in formula (9).

$$\phi_T = \phi_{Tc} e^{-\frac{t}{\tau}} \tag{9}$$

According to formula (7) and (9), the flux at both ends of the transformer is:

$$\phi = \phi_s + \phi_T = \phi_m \cos\omega t + \phi_{Tc} e^{-\frac{t}{\tau}} \tag{10}$$

In formula (10), ϕ_{Tc} and τ can be obtained through test data. Taking the maximum point and the corresponding time of the maximum point of each cycle in the flux curve, and the obtained data is shown in Table 2.

The flux attenuation curve can be obtained by fitting the data in Table 2. Since the transient flux decays exponentially,

TABLE 2. The value and corresponding time of transient flux at the extreme point of steady magnetic flux.

t/s	ϕ/Wb	$ln\phi/Wb$	t/s	ϕ/Wb	$ln\phi/Wb$
0	224.7	5.415	0.46	96.6	4.571
0.02	213.7	5.365	0.48	94	4.543
0.04	203.6	5.316	0.5	91.6	4.517
0.06	194.4	5.27	0.52	89.3	4.492
0.08	185.8	5.225	0.54	87	4.466
0.1	177.9	5.181	0.56	84.9	4.441
0.12	170.6	5.139	0.58	82.8	4.416
0.14	163.7	5.098	0.6	80.9	4.393
0.16	157.3	5.058	0.62	79	4.396
0.18	151.4	5.02	0.64	77.2	4.346
0.2	145.8	4.982	0.66	75.5	4.324
0.22	140.6	4.946	0.68	73.9	4.303
0.24	135.7	4.91	0.7	72.3	4.281
0.26	131	4.875	0.72	70.8	4.26
0.28	126.7	4.842	0.74	69.3	4.238
0.3	122.6	4.809	0.76	67.9	4.218
0.32	118.7	4.777	0.78	66.5	4.197
0.34	115	4.745	0.8	65.2	4.177
0.36	111.5	4.714	0.82	64	4.159
0.38	108.2	4.684	0.84	62.8	4.14
0.4	105.1	4.655	0.86	61.6	4.121
0.42	102.1	4.626	0.88	60.5	4.103
0.44	99.3	4.598	0.9	59.4	4.084

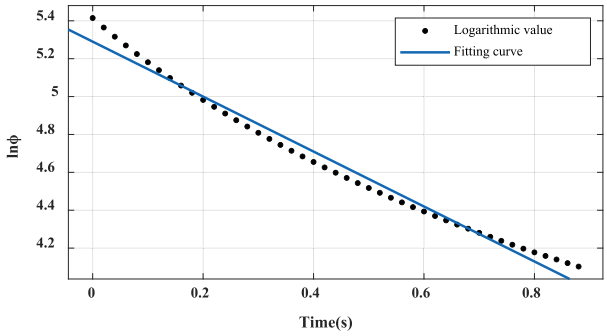

FIGURE 8. Linearization fitting curve of transient flux.

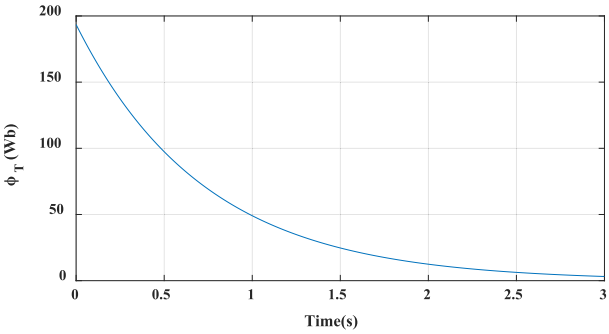

FIGURE 9. Fitting curve transient flux attenuation.

take the logarithm of both sides of formula (9):

$$ln\ \phi_T = ln\ \phi_{Tc} + ln\ e^{-\frac{t}{\tau}} = ln\ \phi_{Tc} + \left(-\frac{t}{\tau}\right) = c_0 + c_1 t \tag{11}$$

It can be seen from Fig. 8 that the logarithm of the transient flux and the time corresponding to the extreme point of the transformer flux are near the straight line $y = c_0 + c_1 t$. Where $c_0 = 5.265$, $c_1 = -1.372$, and $\phi_{Tc} = e^{5.625}$, $\tau = 1/1.372$.

From formulas (9) and (11), the expression of transient flux is: $\phi_T = e^{5.265} e^{-1.372t}$, and the transient flux attenuation curve is shown in Fig. 9.

The flux at both ends of the transformer can be obtained by substituting the fitted transient flux expression into formula (11):

$$\phi = e^{5.265} e^{-1.372t} + \phi_m \cos 100\pi t \tag{12}$$

According to formula (12), the fitting curve of excitation flux attenuation is shown in Fig. 10.

Under the influence of the transient flux, the on-board transformer will enter the saturation state. According to Fig. 11, the on-board transformer will be in the saturation state and the unsaturated state in one cycle. When the flux of the on-board transformer is higher than the saturation flux, it will be in the saturation region. At this time, the excitation inductance is L_{mb}. When the flux of the on-board transformer is lower than the saturation flux, as shown in the shaded part in Fig. 11, it is in the linear region, and the excitation inductance at this time is L_{mx}.

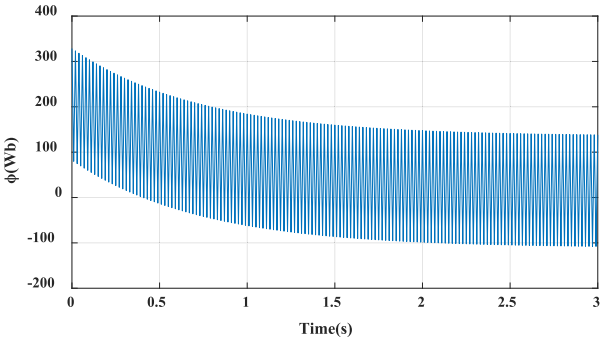

FIGURE 10. Fitting curve of excitation flux attenuation.

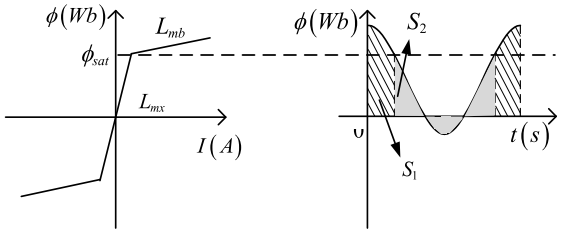

FIGURE 11. Equivalent excitation inductance of on-board transformer.

The equivalent excitation inductance of the transformer can be obtained according to the principle of area equivalence. In a cycle, if the area of the excitation flux is S_1 when it is higher than the saturation flux, S_2 when it is lower than the saturation flux, and the area enclosed by the excitation flux curve and the saturation flux curve is S. Then the equivalent inductance of the transformer in one cycle L_{mdy} is:

$$L_{mdy} = \frac{S_1}{S} L_{mb} + \frac{S_2}{S} L_{mx} \tag{13}$$

Due to the value of excitation inductance is affected by the instantaneous current and the instantaneous magnetic flux, it will change in a cycle. Therefore, the saturation of on-board transformer k_b is defined to evaluate the impact of excitation inductance on system stability. The ratio of saturation area S_1 to total area S is defined as the saturation of transformer k_b, and the expression of saturation is:

$$k_b = \frac{S_1}{S} \tag{14}$$

Saturation of transformer in one cycle is:

$$k_b = 1 - \frac{S_2}{S} = 1 - \frac{\int_{t_1}^{t} 2 \left| \phi_{Tc} e^{-\frac{t}{\tau}} + \phi_m \cos \omega t \right| dt}{\int_{0}^{t} \left| \phi_{Tc} e^{-\frac{t}{\tau}} + \phi_m \cos \omega t \right| dt} \tag{15}$$

Formula (13) can be rewritten as:

$$L_{mdy} = k_b L_{mb} + (1 - k_b) L_{mx} \tag{16}$$

And the excitation flux of the transformer decays exponentially:

$$\phi = \phi_{Tc} e^{-1.372t} + \phi_m \cos 100\pi t = \phi_{sat} \tag{17}$$

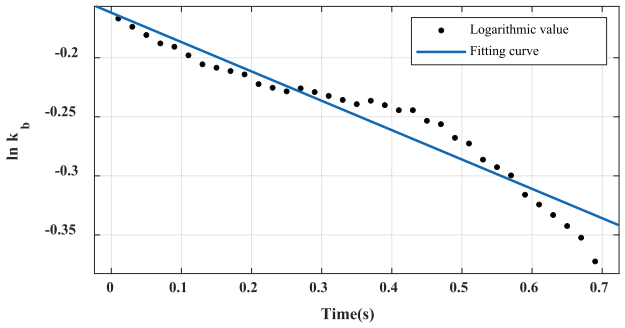

FIGURE 12. Proportion linearization curve.

Since the excitation flux decays exponentially, the saturation also decays exponentially, let:

$$k_b = \mathrm{A}e^{-\alpha t} \tag{18}$$

Take the logarithm of both sides of formula (18) at the same time:

$$ln\, k_b = ln\, A + ln\, e^{-\alpha t} = ln\, A + (-\alpha t) = b_0 + b_1 t \tag{19}$$

It can be seen from Fig. 12 that the logarithm of the transient flux and the time corresponding to the extreme point of the transformer flux are near the straight line $y = -0.1619 - 0.2486t$.

Therefore, the expression of the proportion changing over time is: $k_b = e^{-0.1619}e^{-0.2486t}$, and the change curve of the proportion is shown in Fig. 12. According to formula (16), the equivalent excitation inductance of on-board transformer changes continuously with the attenuation of transient flux.

B. MECHANISM ANALYSIS OF LFO IN VEHICLE-GRID COUPLING SYSTEM

According to the modeling in section II, the vehicle-grid coupling system can be divided into traction power supply system and electric locomotive. It is more complicated to directly analyze the stability of the vehicle-grid coupling system. In this section, on the basis of Middlebrook impedance ratio criterion, the vehicle-grid coupling system is equivalent to a cascade system, as shown in Fig. 2. The equivalent impedance of the traction network is the front output module, and the electric locomotive is the rear input module. The closed-loop transfer function of the vehicle-grid coupling system is:

$$G(s) = \frac{u_n}{u_s} = \frac{1}{1 + Z_o(s)/Z_{ind}(s)} \tag{20}$$

In formula (20), the equivalent open-loop transfer function is:

$$L(s) = Z_o(s)/Z_{ind}(s) \tag{21}$$

According to Middlebrook's impedance ratio criterion, in order to maintain the stability of the cascade system, $|L(s)| \ll 1$ must be satisfied, that is, the amplitude frequency characteristic curve of $L(s)$ should be less than 0dB in the Bode diagram. The rear input impedance of the cascade system is affected by the on-board transformer. In the locomotive equivalent impedance control block diagram, when the on-board transformer is in the linear zone, $G_8 = 1/L_{mx}$; When the on-board transformer is in the saturation area, $G_8 = 1/L_{mb}$. The equivalent impedance of the load is:

$$Z_{ind} = Z_{inx} * \left(1 - \bar{k}_b\right) + Z_{inb} * \bar{k}_b \tag{22}$$

wherein, Z_{inx} is the equivalent input impedance of the electric locomotive when transformer is not saturated, Z_{inb} is the equivalent input impedance of the electric locomotive when transformer is saturated and $\bar{k}_b$ is the average saturation of on-board transformer. According to formula (1), $Z_o(s)$ is the impedance of the traction transformer and traction network line, which will not change. Therefore, the stability of the vehicle-grid coupling system is affected by the rear input impedance of cascade system. According to formula (22), the rear input impedance is affected by the average saturation and control parameters, which will be analyzed below.

TABLE 3. Average saturation of transformer in different time periods.

Time period	$[0, T]$	$[T, 2T]$	$[2T, 3T]$	$[3T, 4T]$	$[4T, 5T]$
$\bar{k}_b$	0.835	0.813	0.797	0.789	0.776

1) STABILITY ANALYSIS INFLUENCED BY THE AVERAGE SATURATION OF ON-BOARD TRANSFORMER

The saturation of on-board transformer will affect the equivalent impedance of locomotive, and then affect the stability of the system. It can be seen from Fig. 9 that the transient flux of the transformer decays exponentially. The decay is fast in the early stage of exponential decay, and it takes a long time to decay to a stable value. After 3τ, the transient flux decays by 99.5%, which can be considered that the transient flux has little effect on the transformer. In the process of excitation flux attenuation, the equivalent impedance of electric locomotive changes constantly. Based on the sliding window theory, the saturation of the on-board transformer is equivalent in different time periods. If the average saturation of the on-board transformer is calculated every five cycles at power frequency, then $T = 0.1s$. The average saturation of the on-board transformer in each time period can be calculated, and the average saturation of the on-board transformer $\bar{k}_b$ in $[0, T]$ can be calculated:

$$\bar{k}_b = \frac{\int_{t_1}^{t_2} \phi dt + \int_{t_3}^{t_4} \phi dt + \cdots + \int_{t_{n1}}^{t_{n2}} \phi dt}{\int_0^{\frac{\tau}{7}} |\phi|\, dt} = 0.835 \tag{23}$$

According to formula (17), 68 intersections of magnetic flux and steady magnetic flux can be obtained, which is the solution of formula (17) in [0, T]. Set these solutions to $t_1, t_2 \ldots t_{n2}$, similarly, the average saturation of transformer in other time periods can be calculated, and only the average saturation in each time period within $[0, 5T]$ is shown in Table 3.

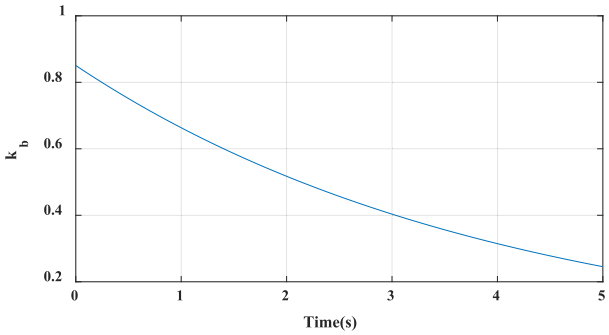

FIGURE 13. Fitting curve of saturation attenuation.

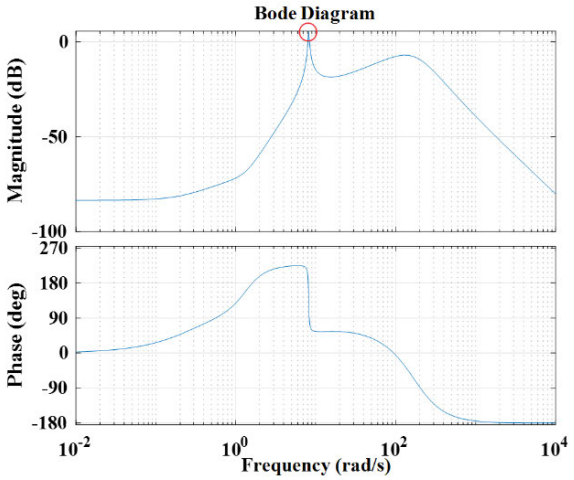

FIGURE 14. Bode diagram of open loop transfer function L(s) at saturation $\bar{k}_b = 0.835$.

It can be seen from table 3 that $\bar{k}_b = 0.835$ in $[0, T]$, and the Bode diagram of the equivalent open-loop transfer function $L(s)$ of the vehicle-grid coupling system is shown in Fig. 14.

It can be seen from Fig. 14 that there is a peak in the amplitude frequency characteristic curve of the system in the low frequency band, and the amplitude corresponding to the peak is greater than 0dB. According to Middlebrook criterion that the LFO will occur in the vehicle-grid coupling system.

With the attenuation of the transient flux, the average saturation of the transformer decreases, the equivalent impedance of the electric locomotive increases, and the output impedance remains unchanged. The frequency characteristic curves under different average saturations are shown in Fig. 15.

By comparing Fig. 15(a) and Fig. 15(b), it can be seen that with the decrease of the average saturation $\bar{k}_b$ of the on-board transformer, the amplitude-frequency characteristic curve of Z_{ind} moves up, and the system gradually tends to be stable. Therefore, with the decay of the transient magnetic flux, the oscillation amplitude of the vehicle-grid coupling system becomes smaller and smaller, and finally tends to be stable.

As the average saturation of the transformer decreases, the equivalent input impedance increases. There must be a $\bar{k}_b$ so

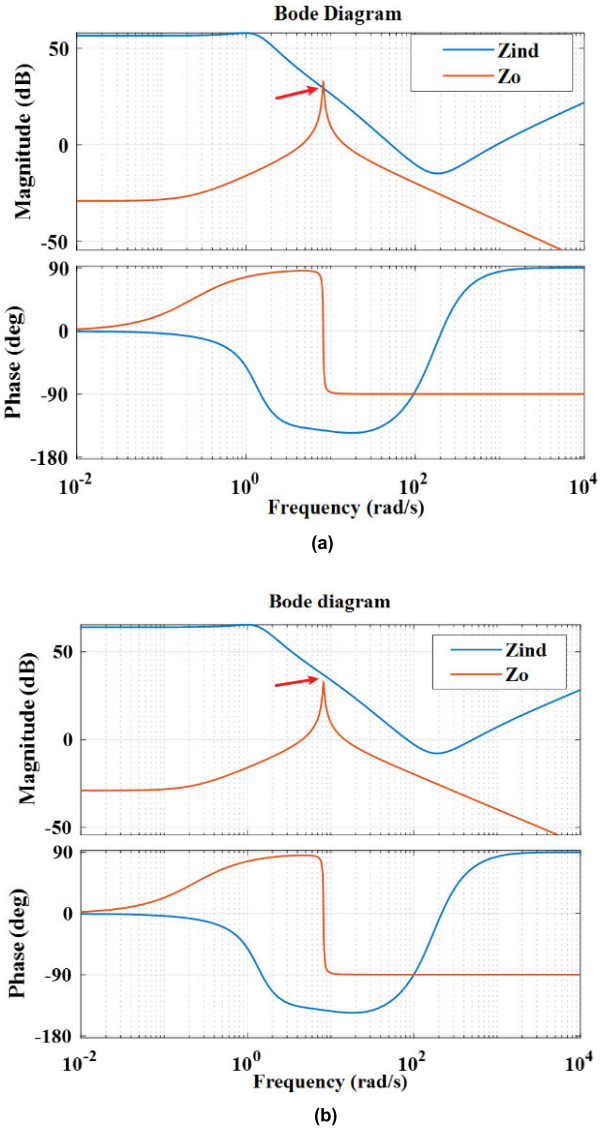

FIGURE 15. Frequency response curve of vehicle-grid coupling system with different average saturation. (a) $\bar{k}_b = 0.797$ (b) $\bar{k}_b = 0.5$.

that the equivalent output impedance is equal to the equivalent input impedance, as shown in formula (24).

$$Z_o = Z_{ind} = Z_{inx} * \left(1 - \bar{k}_b\right) + Z_{inb} * \bar{k}_b \tag{24}$$

The solution is $\bar{k}_b = 0.675$. When the system is critically stable, the amplitude-frequency characteristic curve of $Z_{ind}(s)$ and the maximum value of the amplitude-frequency characteristic curve of $Z_o(s)$ intersect at a point. The frequency ω_r at the intersection is determined by $Z_o(s)$. The equivalent impedance of the traction network is shown in Formula (25), then the amplitude of its frequency domain impedance is:

$$|Z_0(\omega)| = \frac{\sqrt[2]{\left(\omega^2 C^2\right) + \left(R_T + R_{eq}\right)^2}}{\sqrt[2]{1 + \omega^4 \left(L_T + L_{eq}\right)^2 C - 2\omega^2 \left(L_T + L_{eq}\right) C - \omega^2 \left(R_T + R_{eq}\right) C}} \tag{25}$$

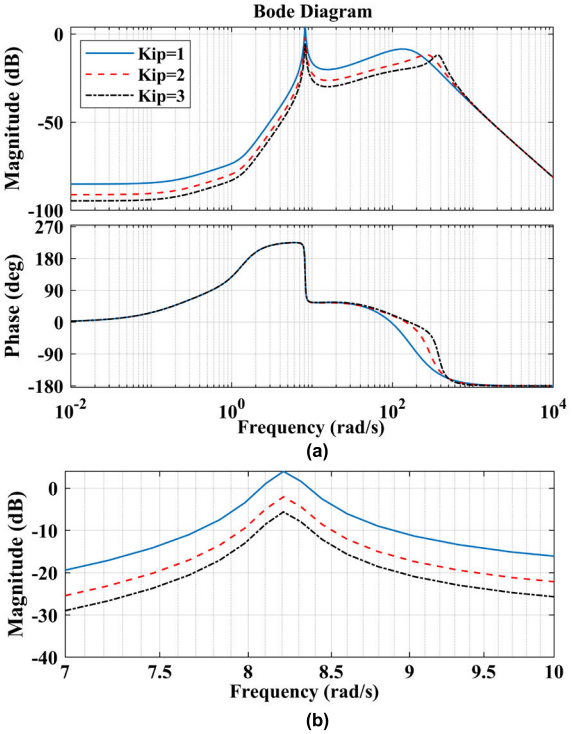

FIGURE 16. Influence of current loop parameters on stability. (a) proportional Parameters (b) zoom-in view of Bode diagram.

When the amplitude of $Z_o(s)$ is the largest, formula (25) holds.

$$\frac{d\,|Z_0(\omega)|}{d\omega} = 0 \tag{26}$$

At this time, $\omega_r = 8.21(rad/s)$, and the oscillation frequency of the system is 1.31Hz.

2) INFLUENCE OF CONTROL PARAMETERS ON STABILITY

The control parameters of electric locomotive will affect the equivalent impedance of locomotive. In this section, the influence of current loop parameters and voltage loop parameters on the stability of vehicle-grid coupling system will be analyzed respectively.

The Bode diagram of the open-loop transfer function of the system is obtained by changing K_{ip}, as shown in Fig. 16. When the proportional coefficient of the current loop decreases, the peak value of the amplitude frequency characteristic curve of the system in the low frequency band rises and tends to cross 0dB. The peak value of the amplitude frequency characteristic curve in the middle frequency band moves to the left and rises, and the system becomes more and more unstable.

The Bode diagram of the open-loop transfer function of the vehicle-grid coupling system is obtained by changing the parameters K_{vp} and K_{vi} of the locomotive equivalent resistance, as shown in the figure below.

As shown in Fig. 17(a) and (b), with the increase of the voltage outer loop proportional coefficient K_{vp}, the amplitude frequency curve moves down in the low frequency band,

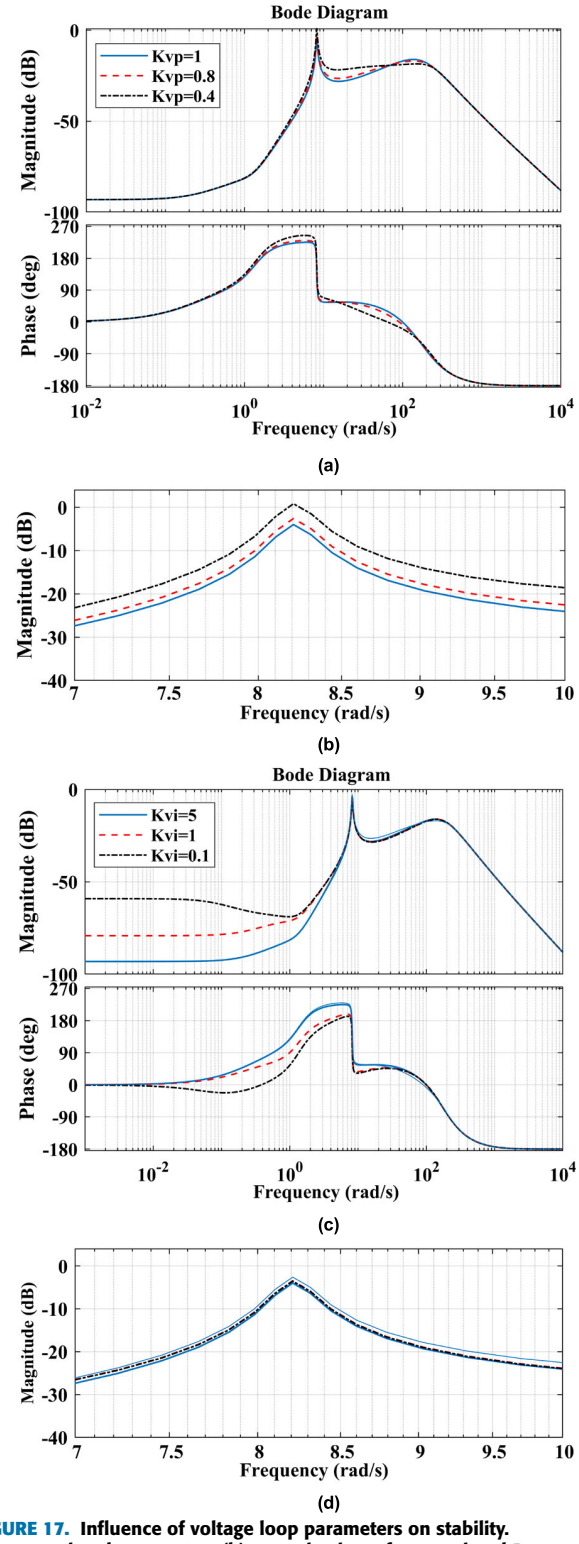

FIGURE 17. Influence of voltage loop parameters on stability. (a) proportional parameters (b) zoom-in view of proportional Parameters Bode diagram (c) integral parameters (d) zoom-in view of integral parameters Bode diagram.

and the system becomes more and more stable. As shown in Fig. 17(c) and (d), the increase of the voltage loop integral parameter K_{vi} has little effect on the vehicle-grid coupling system.

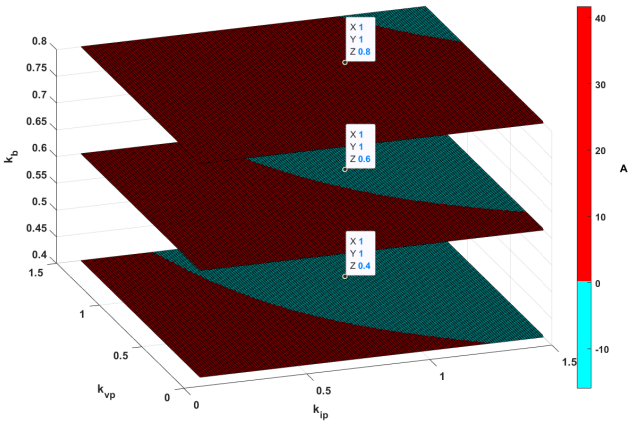

FIGURE 18. Influence of $\bar{k}_b$ on system stability.

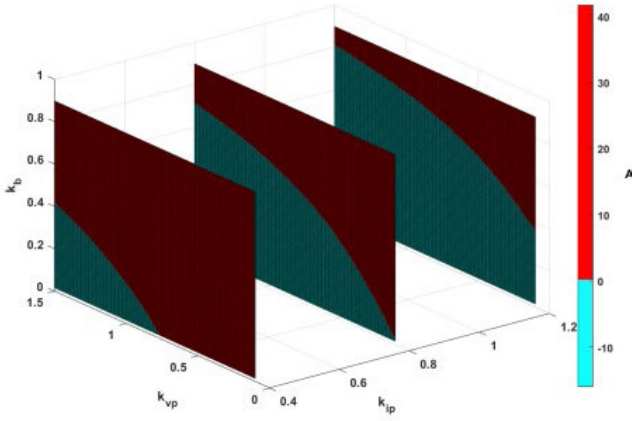

FIGURE 19. Influence of K_{ip} on system stability.

3) STABILITY REGION OF VEHICLE-GRID COUPLING SYSTEM

According to the analysis in the previous two sections, the average saturation of on-board transformer of electric locomotive $\bar{k}_b$, current loop control parameter K_{ip} and voltage loop control parameter K_{vp} has a great impact on the stability of the system. This section will comprehensively analyze their impact on the stability.

According to formula (24) and formula (25), the system is stable when $|L(s)| < 1$. Let $A = 20log\,|L(s)|$, combined with formula (1), formula (20) and formula (22), we can obtain:

$$A = 20\log\left|\frac{\left(Z_T + Z_{eq}\right) / \left[1 + s\left(Z_T + Z_{eq}\right) C\right]}{\left(Z_{inx} * (1 - \bar{k}_b) + Z_{inb} * \bar{k}_b\right)}\right| \tag{27}$$

Z_{inx} and Z_{inb} are greatly affected by locomotive control parameter K_{ip} and K_{vp}. When other parameters are constant, A is a function of $\bar{k}_b$, K_{ip} and K_{vp}, which contains three variables, so the image is a three-dimensional thermodynamic diagram, where the x, y, z axes represent K_{ip} K_{vp} and $\bar{k}_b$, and the color axis indicates the size of A. To facilitate observation, the diagram is sliced along the x, y and z axes, and a three-dimensional thermodynamic diagram is obtained. Take the z-axis as an example, slice along z-axis when $\bar{k}_b$ =0.4, 0.6, 0.8 to obtain Fig. 18. In this figure, the red area indicates $A > 0$, the system is unstable. The light blue area indicates $A < 0$, the system is stable.

As shown in Fig. 18, when $\bar{k}_b$ becomes smaller and smaller, the stability area of the system becomes larger and larger. When K_{ip} =1, K_{vp} =1, if $\bar{k}_b$ =0.8, the system is unstable, and if $\bar{k}_b$ decreases to 0.6, the system is stable.

Similarly, slice along the x-axis when K_{ip} =0.4, 0.8, 1.2 to obtain Fig. 19.

Slice along the y-axis, when K_{vp} =0.4, 0.8, 1.2 to obtain Fig. 20.

As shown in Fig. 19 and Fig. 20, with the increase of K_{ip} and K_{vp}, the stable area of the system becomes larger and larger.

According to Fig. 18, Fig. 19, Fig. 20 and impedance ratio criterion, the system is stable when $\bar{k}_b$, K_{ip}, K_{vp} satisfy the following formula:

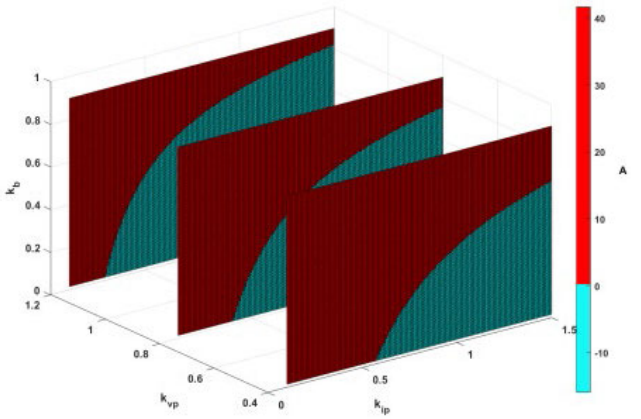

FIGURE 20. Influence of K_{vp} on system stability.

$$\left|\begin{array}{l} -k_b\left\{\begin{array}{l} k_{ip}\left[k_{vp}\left(3.02 - j2.42\right) - 0.47 - j1.8\right] \\ \left(0.055 - j0.002\right) + 0.00009 + j0.0456 \end{array}\right\} \\ + \left(k_b - 1\right)\left\{\begin{array}{l} k_{ip}\left[k_{vp}\left(3.02 - j2.4\right) - 0.47 - j1.8\right] \\ \left(4.3 - j27.59\right) + j2.26 \end{array}\right\} \end{array}\right| < 44 \tag{28}$$

Therefore, the vehicle-grid coupling system can be stabilized by controlling the value of $\bar{k}_b$, K_{ip}, K_{vp}. The value of K_{ip}, K_{vp} can be realized by improving the control strategy of electric locomotive. The value of $\bar{k}_b$ is related to the initial value of the transient flux of the on-board transformer. According to formula (8), ϕ_{Tc} is determined by α and ϕ_r, ϕ_r is related to the opening phase angle of on-board transformer β. Therefore, ϕ_{Tc} jointly determined by α and β when the electric locomotive passes the neutral-section, as shown in formula (29).

$$\phi_{Tc} = \phi_m cos\alpha - \phi_m \cos\beta \tag{29}$$

When $\bar{k}_b = 0.675$, the vehicle-grid coupling system is in a critical stable state, and the average saturation of the on-board

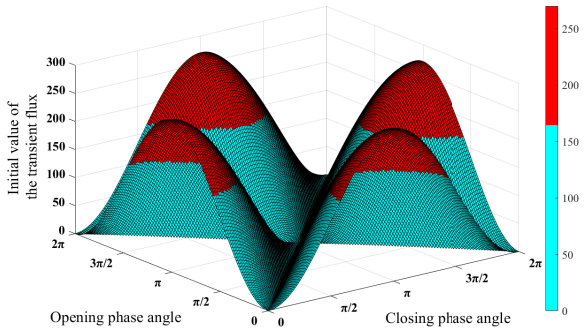

FIGURE 21. Opening and closing phase angle area.

transformer is shown in formula (30):

$$\bar{k}_b = \frac{\lambda e^{-\frac{t_1}{\tau}} + \lambda e^{-\frac{t_2}{\tau}} + \cdots + \lambda e^{-\frac{t_n}{\tau}}}{n} = 0.675 \tag{30}$$

Here $\lambda e^{-\frac{t_1}{\tau}} = 0.7372$, so when the saturation ratio of the first cycle is 0.7372, the vehicle-grid coupling system is in a critical stable state, and the flux of the transformer satisfies formulas (31) and (32).

$$\phi = \phi_{Tc} e^{-1.372t} + \phi_m \cos 100\pi t = \phi_{sat} \tag{31}$$

where $t \in (0, 0.02)$.

$$\frac{\int_{t_1}^{t_2} (\phi_{Tc} e^{-\alpha t} + \phi_m \cos \omega t) dt}{\int_0^t \left| \phi_{Tc} e^{-\alpha t} + \phi_m \cos \omega t \right| dt} = 0.7372 \tag{32}$$

According to the simultaneous formula (31) and formula (32), we can obtain: $\phi_{Tc} = 162$, that is, when the transient flux is 162Wb, the vehicle-grid coupling system is in a critical stable state. In order to maintain the stability of the vehicle-grid coupling system, the initial value of the transient flux must be less than 162Wb, that is, the absolute value of the transient flux at the closing time must less than the transient flux at the critical stable time of the system.

$$|\phi_{Tc}| = \phi_m \, |cos\alpha - \cos \beta| < 162 \tag{33}$$

The relationship between the opening and closing phase angle and the transient flux is shown in Fig. 21. The red part represents that the absolute value of the initial value of the transient flux is greater than 162Wb, and the blue part represents that the absolute value of the initial value of the transient flux is less than 162Wb.

According to Fig. 21 and formula (33), LFO can be suppressed by controlling closing phase angle and opening phase angle when pass the neutral-section, to make the absolute value of the initial value of the transient flux less than 162Wb. The optimal solution is:

$$\alpha = \beta or \alpha + \beta = 2\pi \tag{34}$$

At this time, the transient flux is zero, the transformer will not be saturated, and the system is stable.

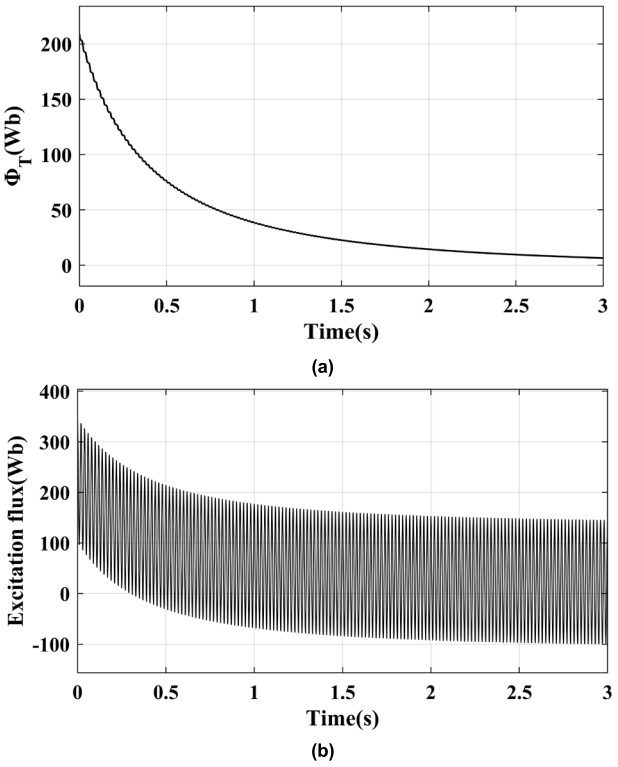

FIGURE 22. Simulation curve of magnetic flux attenuation. (a) transient flux attenuation curve (b) Excitation flux attenuation curve.

IV. SIMULATIONS

In this section, a simulation platform is built in MATLAB/Simulink to verify the correctness of mechanism analysis and stability region. It can be seen from the analysis in Section III-B that when the electric locomotive passes the neutral-section, it will cause the saturation of the on-board transformer, thus reducing the equivalent impedance of the electric locomotive, making the impedance of the vehicle-grid coupling system mismatched, and causing LFO of the voltage and current of the traction network and the locomotive.

A. VERIFICATION OF TRANSIENT FLUX ATTENUATION

When the closing phase angle is 0 degrees and the remanence is 1p.u., the transient flux is maximum. At this time, the flux curve of the locomotive transformer is shown in the following figure.

Comparing Fig. 9 and Fig. 22(a), Fig.10 and Fig. 22(b) respectively, the simulation curve of transient flux attenuation is basically consistent with the fitting curve, which verifies the correctness of exponential attenuation of transient flux.

B. MECHANISM ANALYSIS AND VERIFICATION

When the electric locomotive passes the neutral-section, it will cause the saturation of the on-board transformer, thus reducing the equivalent impedance of electric locomotives and mismatching the impedance of vehicle-grid coupling

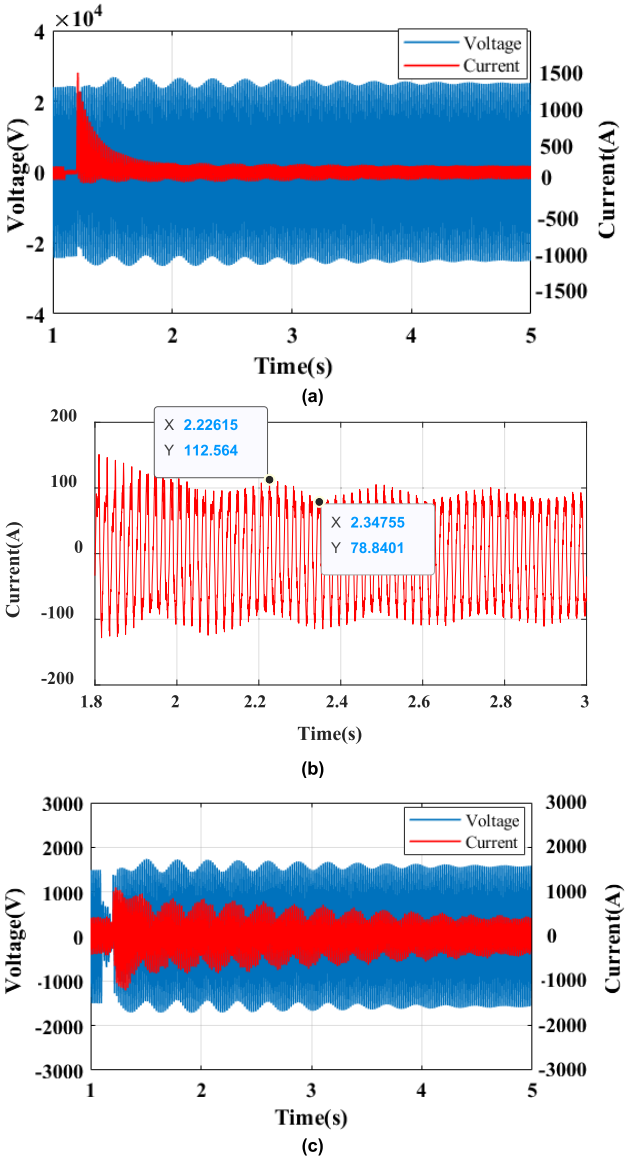

FIGURE 23. LFO waveforms at high saturation. (a) voltage and current waveforms of traction network (b) zoom-in view of current waveform of traction network (c) voltage and current waveforms of electric locomotive.

system, resulting in LFO of voltage and current between traction network and locomotives. The LFO waveforms are shown in Fig. 23.

The electric locomotive passes the neutral-section at 1.1s and reclosed at 1.2s. As can be seen from Fig.23 (a) and (b), voltage drop occurs in traction network at the moment of reclosing, and inrush current is large. In addition, LFO appeared in the voltage and current of the traction network, with the voltage fluctuation range of 13.6% and the current fluctuation range of 42.8%. If there is a heavy-load electric locomotive running under the same power supply arm at this time, it is easy to cause misoperation of feeder impedance protection of traction substation. It can be seen from Fig. 23(c) that the vehicle side voltage fluctuates in

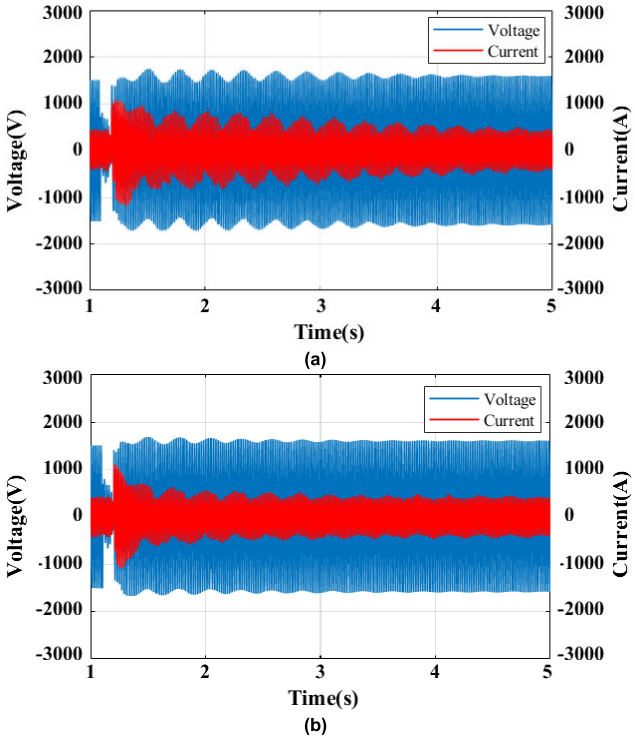

FIGURE 24. Voltage and current waveforms of electric locomotive with different on-board transformer saturation. (a) high saturation (b) low saturation.

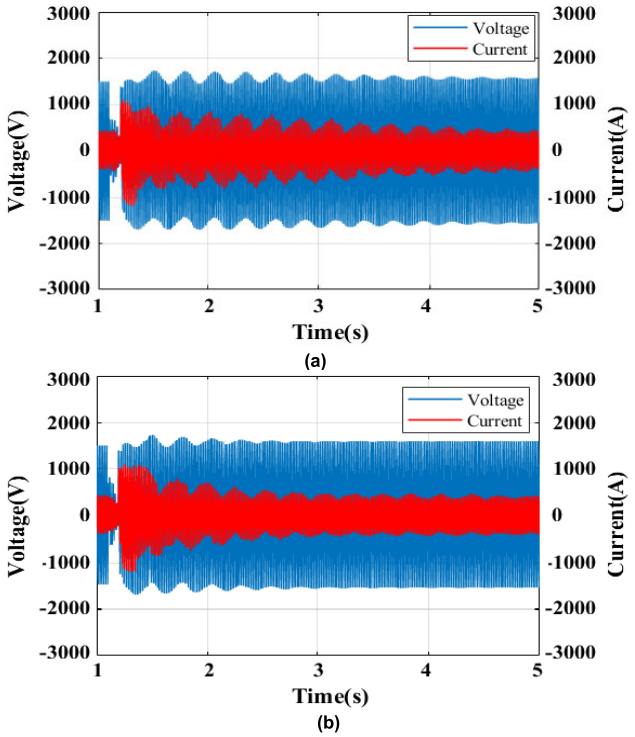

FIGURE 25. Voltage and current waveforms of electric locomotive under different K_{ip}. (a) $K_{ip} = 0.5$ (b) $K_{ip} = 1$.

the range of 1400 ∼ 1750V, with a fluctuation range of 22.6%, which will cause train traction blockade and seriously endanger the driving safety.

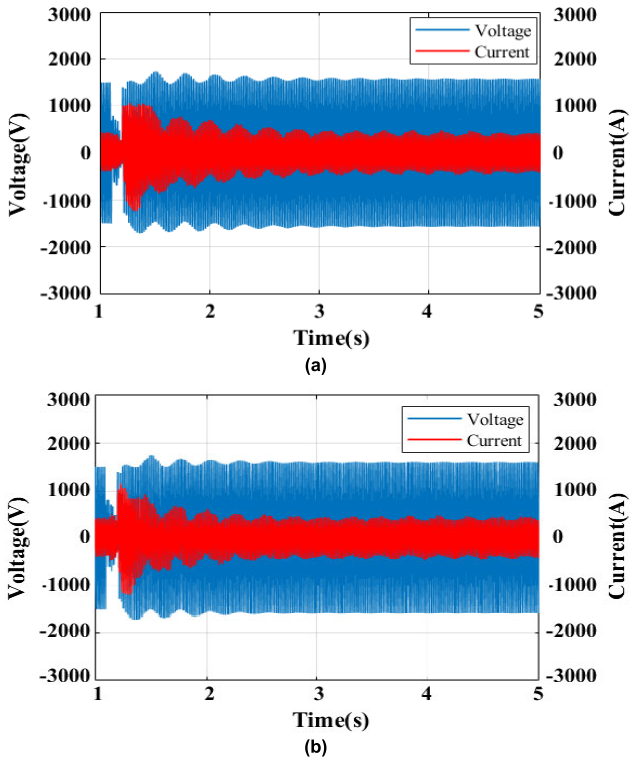

FIGURE 26. Voltage and current waveforms of electric locomotive under different K_{vp}. (a) $K_{vp} = 0.2$ (b) $K_{vp} = 0.4$.

The influence of on-board transformer saturation and control parameters of electric locomotive on LFO is verified as follows.

1) INFLUENCE OF ON-BOARD TRANSFORMER SATURATION

When the electric locomotive passes the neutral-section, due to the different closing phase angles, the on-board transformer will be saturated to different degrees. The simulation waveforms of traction network voltage with different saturation degrees of the transformer are shown in Fig. 24.

According to the simulation results, the saturation of the on-board transformer will cause LFO of the vehicle-grid coupling system. Moreover, the higher the saturation of the on-board transformer, the stronger the oscillation. After the oscillation occurs, the amplitude decreases gradually. Compared with the previous analysis, the saturation of on-board transformer decreases with the decay of transformer transient magnetic flux. When the saturation of on-board transformer decreases to the critical value, the vehicle-grid coupling system returns to stability.

2) INFLUENCE OF CONTROL PARAMETERS

According to the previous analysis, among the control parameters of electric locomotive, the proportion parameters of the current inner loop and the control parameters of the voltage outer loop have a great impact on the system. The following simulation mainly verifies the impact of K_{ip} and K_{vp} on the system stability. Change parameter K_{ip}, the voltage and current waveforms of electric locomotive are shown in Fig. 25,

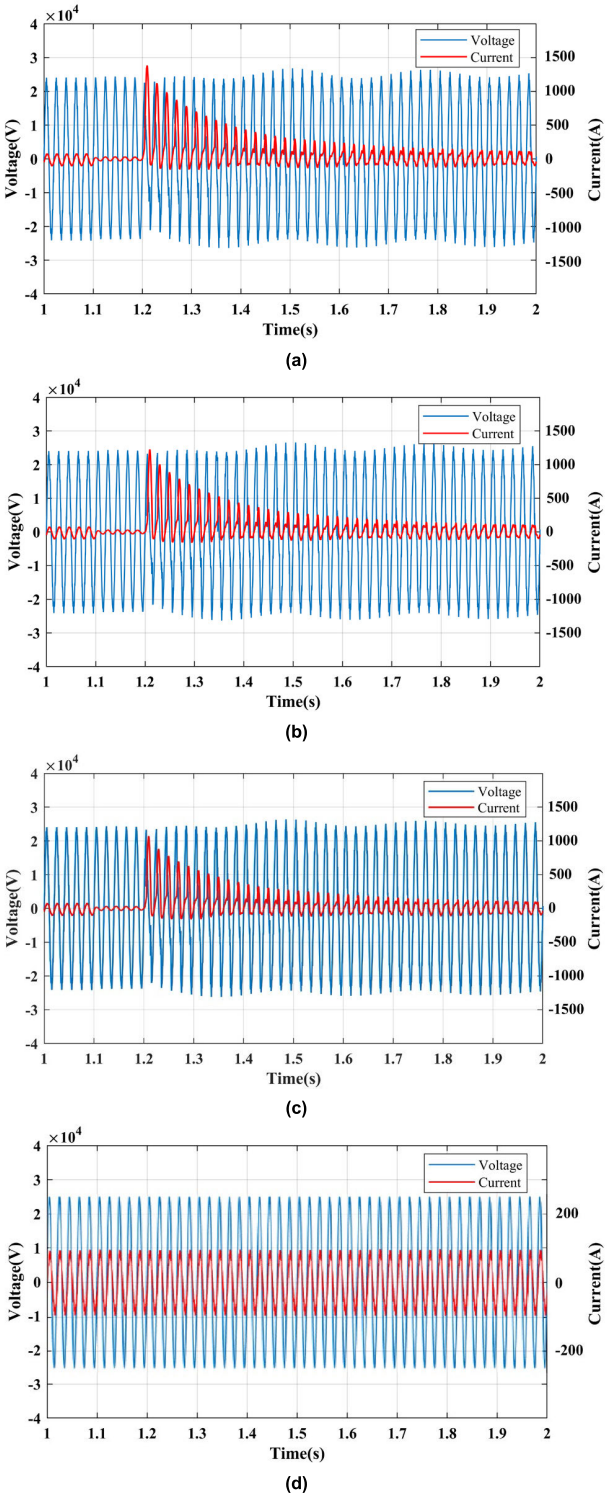

FIGURE 27. Waveforms of traction network before and after closing phase angle adjustment. (a) closing phase angle in unstable region, $\alpha = 0$ (b) closing phase angle in unstable region, $\alpha = \frac{\pi}{6}$ (c) closing phase angle in unstable region, $\alpha = \frac{\pi}{4}$ (d) closing phase angle is optimal.

and change parameter K_{vp}, the voltage and circuit waveforms of electric locomotive are shown in Fig. 26.

Comparing Fig. 25(a) and Fig. 25(b), it can be seen that with the increase of K_{ip}, the oscillation of voltage and current

is weakened, which verifies the previous analysis and also proves that LFO can be suppressed by changing the current loop control parameters.

Comparing Fig. 26(a) and Fig. 26(b), it can be seen that with the increase of K_{vp}, the oscillation of voltage and current is weakened, which verifies the previous analysis and also proves that LFO can be suppressed by changing the voltage loop control parameters.

According to the previous analysis, LFO can be effectively suppressed by controlling the opening and closing phase angle. By comparing the voltage and current waveforms at the grid side of the electric locomotive between the normal phase transition and the phase-selecting closing phase transition, the simulation verifies the suppression effect of LFO. The simulation results are shown in Fig. 27.

It can be seen from Fig. 27(a), (b) and (c) that the inrush current will be generated when the closing phase angle of the electric locomotive is in the unstable area, and the instantaneous amplitude of the inrush current can reach 1500A. The voltage of the traction network will drop at the moment of closing, and the voltage and current of the traction network will oscillate about 2-3Hz. In addition, as the closing phase angle approaches the stable region, the inrush current and the amplitude of voltage fluctuation has decreased significantly. It can be seen from Fig. 27(d) that within the system stability region, when the closing phase angle is optimal, the electric locomotive will not produce excitation inrush current when passing the neutral-section, and the network voltage and current remain stable.

V. CONCLUSION

This paper mainly studies the transient LFO caused by electric locomotive when passing the neutral-section, the nonlinear modeling and mechanism analysis of vehicle-grid coupling system are discussed in details all through the paper. The correctness of presented analysis method is verified by simulation. The main conclusions are as follows:

(1) The influence of instantaneous closing phase angle and residual magnetism on the initial value of transient flux and the attenuation of transient flux are analyzed at the moment of passing the neutral-section. The attenuation curves of transient flux and excitation flux are fitted, and the saturation of on-board transformer is defined. Based on the principle of area equivalence, the function of transformer saturation changing with time is deduced, and the conclusion that excitation inductance changes continuously with the attenuation of transient flux is obtained.

(2) Based on the sliding window theory, the average saturation of the on-board transformer in different periods of time is calculated. Combined with the equivalent circuit model of the electric locomotive, the equivalent frequency domain impedance of the electric locomotive is obtained. Based on Middlebrook impedance ratio criterion, the influence of saturation of on-board transformer and control parameters of electric locomotive on the stability of vehicle-grid coupling system is analyzed. Based on the above analysis, the stability region of the system is obtained when the saturation of the on-board transformer, the proportional control parameters of the voltage loop and the proportional control parameters of the current loop change, and the opening and closing phase angles under the stability of the vehicle-grid coupling system are also defined.

(3) Benefits of system stability region determination: the saturation of the on-board transformer will cause the reduction of locomotive impedance and the instability of the system. The saturation of the on-board transformer is affected by the transient flux, which is related to the closing phase angle and opening phase angle. In addition, the control parameters of the grid side rectifier can affect the equivalent impedance of the locomotive. Therefore, the LFO can be suppressed by controlling the opening and closing phase angles and improving the control strategy of grid side rectifier.

REFERENCES

[1] G.-S. Lee, P.-I. Hwang, B.-G. Lee, and S.-I. Moon, "Loss minimization of electrified railway traction systems using SVC based on particle swarm optimization," *IEEE Access*, vol. 8, pp. 219680–219689, 2020, doi: 10.1109/ACCESS.2020.3042467.

[2] J. Chen, Y. Ge, K. Wang, H. Hu, Z. He, Z. Tian, and Y. Li, "Integrated regenerative braking energy utilization system for multi-substations in electrified railways," *IEEE Trans. Ind. Electron.*, vol. 70, no. 1, pp. 298–310, Jan. 2023, doi: 10.1109/TIE.2022.3146563.

[3] L. Li, M. Wu, S. Wu, J. Li, and K. Song, "A three-phase to single-phase AC-DC-AC topology based on multi-converter in AC electric railway application," *IEEE Access*, vol. 7, pp. 111539–111558, 2019, doi: 10.1109/ACCESS.2019.2933949.

[4] Y. Ge, H. Hu, Y. Huang, K. Wang, J. Chen, and Z. He, "Quadratic sensitivity models for flexible power quality improvement in AC electrified railways," *IEEE Trans. Power Electron.*, vol. 38, no. 3, pp. 2844–2849, Mar. 2023, doi: 10.1109/TPEL.2022.3222183.

[5] H. Bu, Y. Lee, Y. Cho, M.-Y. Kim, E. Lee, and J.-H. Park, "Neutral section passing strategy preventing inrush current for electric railway solid-state transformers," *J. Power Electron.*, vol. 21, no. 8, pp. 1135–1143, Aug. 2021, doi: 10.1007/s43236-021-00261-5.

[6] T. Moore, F. Schmid, and P. Tricoli, "Voltage transient management for alternating current trains with vacuum circuit breakers," *IET Electr. Syst. Transp.*, vol. 12, no. 1, pp. 1–14, Mar. 2022, doi: 10.1049/els2.12034.

[7] H.-S. Shin, S.-M. Cho, J.-S. Huh, J.-C. Kim, and D.-J. Kweon, "Application on of SFCL in automatic power changeover switch system of electric railways," *IEEE Trans. Appl. Supercond.*, vol. 22, no. 3, Jun. 2012, Art. no. 5600704, doi: 10.1109/TASC.2011.2177617.

[8] X. Zhang, J. Chen, R. Qiu, and Z. Liu, "VCT-AOC comprehensive method to suppress high-frequency resonance and low-frequency oscillation in railway traction power supply system," *IEEE Access*, vol. 7, pp. 152202–152213, 2019, doi: 10.1109/ACCESS.2019.2948210.

[9] C. Yao, X. Wang, and C. Bi, "The analysis and modeling of TCSC in the low-frequency oscillation suppression of electrified railway," in *Proc. IEEE 3rd Int. Electr. Energy Conf. (CIEEC)*, Beijing, Sep. 2019, pp. 26–2123, doi: 10.1109/cieec47146.2019.Cieec-2019733.

[10] S. Yang, Y. Wang, K. Song, M. Wu, and G. Konstantinou, "Stability and suppression study for low-frequency oscillations in network-train system," *IEEE Access*, vol. 8, pp. 30575–30590, 2020, doi: 10.1109/ACCESS.2020.2972947.

[11] H. Chen, W. Yu, Z. Liu, Q. Yan, I. A. Tasiu, and Z. Han, "Low-frequency instability induced by Hopf bifurcation in a single-phase converter connected to non-ideal power grid," *IEEE Access*, vol. 8, pp. 62871–62882, 2020, doi: 10.1109/ACCESS.2020.2983479.

[12] Y. Zhang, S. Wu, Z. Liu, Q. Yan, and T. Chen, "An approach to improve system performance in the vehicle-grid system using sliding mode control under multiple operation conditions," *IEEE Access*, vol. 8, pp. 11084–11095, 2020, doi: 10.1109/ACCESS.2020.2965215.

[13] P. Frutos, P. Ladoux, N. Roux, I. Larrazabal, J. M. Guerrero, and F. Briz, "Low frequency stability of AC railway traction power systems: Analysis of the influence of traction unit parameters," *Electronics*, vol. 11, no. 10, p. 1593, May 2022, doi: 10.3390/electronics11101593.
[14] F.-G. Paul, J. M. Guerrero, I. Muniategui-Aspiazu, I. Vicente-Makazaga, A. Endemano-Isasi, D. Ortega-Rodriguez, and F. Briz, "Power-hardware-in-the-loop emulation of the low-frequency oscillation phenomenon in AC railway networks," *IEEE Access*, vol. 10, pp. 87374–87386, 2022, doi: 10.1109/ACCESS.2022.3198945.
[15] C. Bi, X. Wang, C. Yao, K. Pang, and C. Jin, "Analysis and evaluation of suppression methods on low-frequency oscillation in electric railways," in *Proc. IEEE 2nd Int. Electr. Energy Conf. (CIEEC)*, Nov. 2018, pp. 56–63, doi: 10.1109/CIEEC.2018.8745877.
[16] K. Jiang, C. Zhang, and X. Ge, "Low-frequency oscillation analysis of the train-grid system based on an improved forbidden-region criterion," *IEEE Trans. Ind. Appl.*, vol. 54, no. 5, pp. 5064–5073, Sep. 2018, doi: 10.1109/TIA.2018.2838561.
[17] C. Daopin, O. Xiaomei, L. Yue, and W. Zhiqi, "A method based on 2DOF-IMC to voltage low-frequency oscillation suppression in high-speed railway traction network," in *Proc. China Int. Conf. Electr. Distribution (CICED)*, Aug. 2016, pp. 1–5, doi: 10.1109/CICED.2016.7575899.
[18] Y. Hong, Z. Shuai, H. Cheng, C. Tu, Y. Li, and Z. J. Shen, "Stability analysis of low-frequency oscillation in train-network system using RLC circuit model," *IEEE Trans. Transport. Electrific.*, vol. 5, no. 2, pp. 502–514, Jun. 2019, doi: 10.1109/TTE.2019.2905983.
[19] Q. Liu, M. Wu, J. Li, and S. Yang, "Frequency-scanning harmonic generator for (inter)harmonic impedance tests and its implementation in actual 2 × 25 kV railway systems," *IEEE Trans. Ind. Electron.*, vol. 68, no. 6, pp. 4801–4811, Jun. 2021, doi: 10.1109/TIE.2020.2989706.
[20] K. Xi and Z. Li, "Mechanism analysis of sympathetic inrush in traction network cascaded transformer based on flux linkage-current circuit model," in *Proc. 8th Int. Conf. Power Energy Syst. (ICPES)*, Colombo, Sri Lanka, Dec. 2018, pp. 87–92.
[21] H. Lee, C. Lee, G. Jang, and S. Kwon, "Harmonic analysis of the Korean high-speed railway using the eight-port representation model," *IEEE Trans. Power Del.*, vol. 21, no. 2, pp. 979–986, Apr. 2006, doi: 10.1109/TPWRD.2006.870985.
[22] H. Hu, H. Tao, F. Blaabjerg, X. Wang, Z. He, and S. Gao, "Train–network interactions and stability evaluation in high-speed railways–Part I: Phenomena and modeling," *IEEE Trans. Power Electron.*, vol. 33, no. 6, pp. 4627–4642, Jun. 2018, doi: 10.1109/TPEL.2017.2781880.
[23] J. Li and X. Chen, "Mechanism analysis of sympathetic inrush in traction network cascaded transformers based on flux-current circuit model," *Energies*, vol. 12, no. 21, p. 4210, Nov. 2019, doi: 10.3390/en12214210.
[24] Z. Huang, Z. Jia, and Z. Li, "Research on transformer saturation characteristics of electric locomotive based on flux—Current loop model," in *Proc. 9th Int. Conf. Power Energy Syst. (ICPES)*, Perth, WA, Australia, Dec. 2019, pp. 1–6.
[25] S. Danielsen, T. Toftevaag, and O. B. Fosso, "Application of linear analysis in traction power system stability studies," in *Proc. WIT Trans. Built Environ.*, Toledo, Spain, Aug. 2008, pp. 10–401, doi: 10.2495/cr080401.
[26] S. Danielsen, O. B. Fosso, and T. Toftevaag, "Use of participation factors and parameter sensitivities in study and improvement of low-frequency stability between electrical rail vehicle and power supply," in *Proc. 13th Eur. Conf. Power Electron. Appl. (EPE)*, Barcelona, Spain, Sep. 2009, pp. 42–633.
[27] Y. Zhou, H. Hu, X. Yang, J. Yang, Z. He, and S. Gao, "Low frequency oscillation traceability and suppression in railway electrification systems," *IEEE Trans. Ind. Appl.*, vol. 55, no. 6, pp. 7699–7711, Nov. 2019, doi: 10.1109/tia.2019.2935194.
[28] Z. Liu, G. Zhang, and Y. Liao, "Stability research of high-speed railway EMUs and traction network cascade system considering impedance matching," *IEEE Trans. Ind. Appl.*, vol. 52, no. 5, pp. 4315–4326, Sep. 2016, doi: 10.1109/tia.2016.2574770.
[29] J. H. Feng, Z. Chen, Z. Zhang, W. Luo, and L. Su, "The cause analysis for low-frequency oscillation of Ac electric locomotive and traction power supply network," in *Proc. Int. Conf. Elect. Inf. Technol. Rail Transp.*, Zhuzhou, China, Aug. 2015, pp. 597–608, doi: 10.1007/978-3-662-49367-0_59.
[30] X. Zhang, J. Chen, G. Zhang, L. Wang, R. Qiu, and Z. Liu, "An active oscillation compensation method to mitigate high-frequency harmonic instability and low-frequency oscillation in railway traction power supply system," *IEEE Access*, vol. 6, pp. 67–70359, 2018, doi: 10.1109/ACCESS.2018.2879054.
[31] Y. Liao, Z. Liu, G. Zhang, and C. Xiang, "Vehicle-grid system modeling and stability analysis with forbidden region-based criterion," *IEEE Trans. Power Electron.*, vol. 32, no. 5, pp. 3499–3512, May 2017, doi: 10.1109/TPEL.2016.2587726.
[32] H. Wang, W. Mingli, and J. Sun, "Analysis of low-frequency oscillation in electric railways based on small-signal modeling of vehicle-grid system in Dq frame," *IEEE Trans. Power Electron.*, vol. 30, no. 9, pp. 5318–5330, Sep. 2015, doi: 10.1109/TPEL.2015.2388796.

ZHIYONG LI received the B.S. degree from the Nanjing University of Science and Technology, Nanjing, China, in 1994, and the M.S. and Ph.D. degrees from Central South University, Changsha, China, in 2006. From 2007 to 2008, he was a Visiting Scholar with the Power System Laboratory, Swiss Federal Institute of Technology. He is currently an Associate Professor with the Department of Automation, Central South University. His research interests include power system fault prediction and multi-objective optimization in distribution networks.

JIAHUA PI received the B.S. degree from Qingdao University, Qingdao, China, in 2020. He is currently pursuing the M.S. degree in electrical engineering with Central South University, China. His research interests include power quality control in electrified railways and wind power generation.

YUAN CAO received the B.S. and M.S. degrees from Central South University, Changsha, China, in 2011 and 2014, respectively, and the Ph.D. degree from the Department of Electrical and Computer Engineering, The University of Alabama, Tuscaloosa, AL, USA, in 2019, all in electrical engineering. He is currently an Associate Professor with the Department of Automation, Central South University. Before that, he was with Baidu, USA, Hyperloop Technologies, and SANY Group. His research interests include energy storage, battery management systems, and power electronics. He received the Graduate Council Fellowship Award, in 2015 and 2017, respectively. He also received the outstanding student from the College of Engineering, The University of Alabama, in 2018 and 2019.

YEFAN WU received the M.S. degree from Hunan University, China, in 2015. He is currently with State Grid Hunan Electric Power Company Ltd., Economic & Technical Research Institute, Changsha, China. His research interests include power quality, power electronics, and smart-grid planning.

ZHIJIE JIA received the B.S. degree from Northeast Petroleum University, China, in 2018, and the M.S. degree from Central South University, Changsha, China, in 2021. His research interest includes low-frequency oscillation in electrified railways.